Instability of a junction vortex

By J.J.Allen and T.Naitoh

Department of Mechanical and Aerospace Engineering,
Princeton University, Princeton, NJ, 08540, USA

Under consideration for publication in the Journal of fluid mechanics

The flow field in the region where a moving wall, started from rest, slides under a stationary one, produces an interesting flow phenomena with a relatively simple generation geometry. Experiments show that if the wall speed is high enough a vortex forms close to the junction of the moving wall with the stationary one. The experiments described in this paper were conducted over a range of Reynolds numbers from $5\times10^2 \rightarrow 5\times10^5$ where the Reynolds number is defined as $\mathrm{Re}_\Gamma = U_{wall}L/\nu$. This Reynolds number develops during an experiment. U_{wall} is the wall speed and L is the distance moved by the wall. Vortex formation was observed for the full range of Reynolds number. The data reveals that in the absence of an apparatus length scale, the vortical structure appears to scale in a self-similar fashion. The streamwise location of the vortex core, X_Γ, appears to scale directly with the convective length scale, L and independent of Re_Γ. The vertical displacement of the core from the plate surface, Y_Γ, appears to scale as a universal function but with a Re_Γ dependence. Over this large Reynolds number range the vortical structure, which is initially laminar, begins to transition at $\mathrm{Re}_\Gamma \approx 16{,}000$ and appears to be fully turbulent by $\mathrm{Re}_\Gamma \approx 40{,}000$. The transitional regime is marked by the appearance of an instability wave on the perimeter of the vortical structure. The instability mechanism appears to be centrifugal in nature. The formation and non-linear growth of these structures and their ingestion into the primary vortex core is what causes the eventual turbulent breakdown of the primary vortex.

1. Introduction

When a moving wall slides under a stationary one the potential exists for a vortical structure to develop close to the junction of the walls if the moving wall speed is sufficiently high. The impulsively started moving wall drives the Stokes layer, which is essentially a vorticity front, past the singularity at the junction and over the stationary wall. Significant secondary vorticity develops over the stationary wall as a result. The flow field over the stationary wall resembles an unsteady wall jet, which then separates and rolls into a vortical structure. A schematic of the development process is shown in figure 1. From observations of the dye streak line pattern, it appears that the point of "separation" of the boundary layer from the stationary wall is located directly under the primary vortex and moves along the wall as the vortex structure develops. The presence of the separated vortical structure will enhance the adverse pressure gradient on the stationary wall and appears to sustain flow separation. The use of the term "separation" in

this context does not imply zero shear stress but rather the transition between high speed fluid, originally located over the moving wall and slow speed fluid, originally located over the stationary wall. There does not appear to be a region of reversed flow on the stationary wall. A similar point was made in Lichter, Flor & van Heijst (1992).

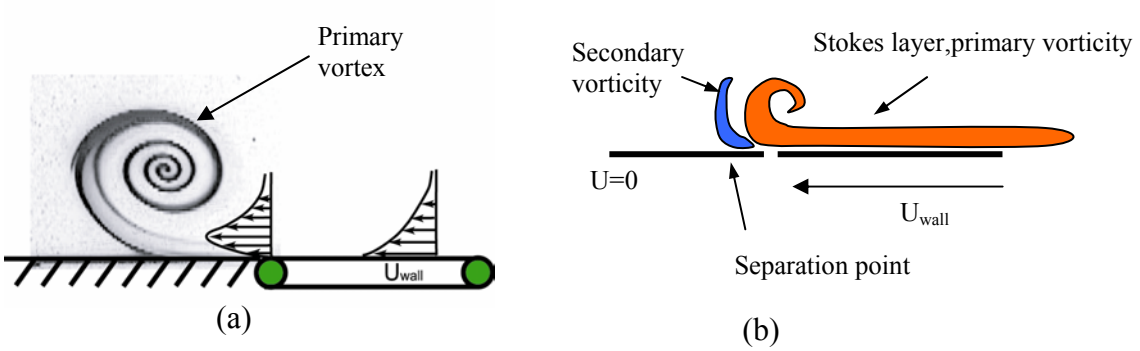

Figure 1(a) Transition of Stokes layer to wall jet (b) Schematic of vorticity generation

This type of vortical structure is generated in a range of industrially significant situations. Most importantly being at the head of a piston as it moves through a cylinder, see Obokata (1992), Guezet and Kageyama (1997) and obviously it effects the turbulent mixing that occurs in an engine cylinder. Another industrially significant situation where this vortex forms is during automobile braking. When surface friction brakes are applied this type of separated structure is formed at the disc/pad junction and affects the rate of brake cooling, see Klein *et al* (2001)

Experimental studies examining the transient development of the structure close to where a moving boundary slides under a stationary one have typically consisted of an apparatus that employs a piston moving through a cylinder resulting in the formation of a vortex ring in front of the piston. Historically the use of a piston/cylinder geometry was motivated by the desire to analyze the flow inside an internal combustion engine. The use of a piston/cylinder apparatus introduces an apparatus length scale, the diameter of the cylinder, to the study of the transient vortical development. In these studies the size of the vortical structure is of the order the cylinder diameter and hence a question exists as to whether the length scale is relevant to the development of the transient structure. Hughes and Gerrard (1971) suggested a minimum Reynolds number for formation of the piston vortex of $\mathrm{Re}_D = U_{wall} D/\nu = 400$, where D is the piston diameter. Tabaczynski *et al* (1970) conducted experiments examining the development of the piston vortex for high values of Re_Γ, of the order $10^3 \rightarrow 10^5$. The piston vortex was present in all their visualizations. Tabaczynski *et al* (1970) identified the transition of the vortex from a laminar to turbulent structure at $\mathrm{Re}_\Gamma \approx 1.5\times10^4$ and suggested self-similar relationships for the spatial growth of the "area" of the vortex in the laminar regime and turbulent regime, when the size of the structure was small in relation to D. No mechanism was suggested for the causes of the transition. Recent experiments of Allen and Chong (2000) measured the strength of the developing vortex structure in front of a piston for Re_Γ in the range of 500-30,000. If one considers the amount of circulation being swept into the

corner as being proportional to $0.5U_{Wall}^2 t$, it was found that the strength of the separated vortex was of the order 25% this value, indicting that significant vorticity cancellation is occurring with the concentrated secondary vorticity that develops on the piston face.

In a wider context this type of vortical structure occurs in shear/lid driven cavity flows. Apart from the obvious practical applications, the study of cavity flows has been motivated by the desire to formulate a model for separated flows at high Reynolds number, see Batchelor (1956) and also serve as a test case for numerical codes. Cavity flows exhibit a range of topologies, dependant on the Reynolds number. Typically the flow is described in terms of a primary eddy and viscous corner eddies, see Pan & Acrivos (1967). The flow is driven by the shear of the motion of the lid (or free stream) and as the Reynolds number increases the primary eddy transitions from viscous in nature, Re~50, to being essentially inviscid by Re~400, see Burgraff (1966). The trend is for the steady state location of the core of the primary eddy to approach the center of the cavity as the Reynolds number increases. If the geometry of the cavity consists of sharp corners, the flow are also marked by the presence of viscous corner eddies. A description of the self-similar structure of these eddies was given by Moffat (1964). A physical description of the mechanism for the formation of these corner eddies was given in Koseff & Street (1984a) as "when the wall jet, that forms on the downstream wall of the cavity, encounters the pressure gradient induced by the corner, separation occurs, resulting in the formation of a secondary eddy in the corner". The streamline separating the inviscid primary vortex and the viscous corner eddy represents a line of high shear and is similar to the region separating primary and secondary vorticity shown in figure 1(b). The recent experiments of Migeon, Texier & Pineau (2000) and Guermond *et al.* (2002) examined the transient development of cavity flows and Migeon *et al.* (2000) concluded that the shallower the cavity the sooner the pressure gradient imposed by the depth of the cavity was felt by the growing corner vortex and the sooner steady state was reached.

The nature of the flow in the immediate junction region where a moving wall slides under a stationary one was considered by Taylor (1962), who developed a steady viscous solution for the stream-function. This solution is often referred to as the "scraping corner solution". As this solution is viscous, it has a very limited physical range. Batchelor (1965) estimates the region of validity for this solution to be of order $rU_{wall}/\nu << 1$ where r is the distance from the corner junction. Some important features of this solution are worthy of comment. At the corner, $r = 0$, the viscous solution is singular in pressure and vorticity. Taylor (1962) noted that the singularity is physically relieved by the presence of a small gap between the plates. The viscous solution does not display any characteristics of the flow separation that occurs during high Reynolds number experiments, nor the decay of the velocity as $r \to \infty$. Hancock, Lewis & Moffat (1981) analyzed the same problem and extended the work of Taylor (1962) to include inertial effects and develop a steady state expression for the self-similar streamfunction that is applicable to a range of the order $5 \approx U_{wall} r / \upsilon$. Hancock *et al* (1981) showed that the resultant velocity profile over the stationary plate with the inertial correction appears somewhat similar to that of a wall jet. Hancock *et al* (1981) also makes the point that there exist homogenous eigenfunction contributions to the non-homogenous solutions that are dependent on boundary conditions distant from the junction.

The fact that the velocity profile over the stationary wall resembles a wall jet provokes the question as to what are the characteristics of unsteady wall jet flows and do they display similar separation phenomena as observed in experiments. Wall jets consist of an inner layer that resembles a wall boundary layer and an outer layer that resembles a free shear layer. Both these layers are unstable at sufficiently high Reynolds number, Chun & Schwartz (1967). The outer layer transitions at the lower Reynolds number. This instability results in the formation of discrete vortical structures in the outer and inner layers. Bajura & Catalano (1975) studied the 'lift-off' of the wall jet from the surface and suggested that this was a result of a dislocation of phase of the instability structures in the inner and outer layer. The streamwise location where lift-off occurred was an order of magnitude greater than the size of the separating structure and the streamwise wavelength of the instability structures. The separation in the current experiments appears to stimulated by a different mechanism, as it is almost instantaneous, compared to the experimental study of Bajura & Catalano (1975).

To the authors knowledge the only study that examines the separation mechanism is that of Conlon & Lichter (1995). They studied the transient start up of a wall jet in the context of explanation of the large separated eddies that are seen in costal currents, see Lichter et al. (1992) and Ahlnas, Roger & George (1987). Conlon & Lichter (1995) made the important distinction that the steady flow case of Bajura & Catalano (1975) and transient start-up, that is the focus of this study, have distinctly different separation mechanisms. The transient flow of Conlon & Lichter (1975) was characterized by the formation of a dipole at the head of the jet. The evolution of this dipole was the dominant feature of the transient flow and they noted that methods of linear stability are not relevant to the description of the transient problem. The features of their simulations, the formation of a separating dipole from the stationary wall surface and the stretching of secondary vorticity around the periphery of the primary vortex have a strong resemblance to the experimental results of the current study and the work of Allen & Chong (2000). The formation of the dipole (vortex) in Conlon & Lichter (1995) was related to an instability that forms on the vorticity front as it enters a region of irrotational flow. Stern & Pratt (1985) studied the evolution of a uniform front of vorticity as it enters a region of irrotational fluid and calculated that an inflectional instability forms behind the nose of the jet, resulting in entrainment into the jet and the formation of a "dipole" structure at the head of the jet. The important result from the work of Conlon & Lichter (1995) was the recognition of the role of the instability of the vortex front in terms of starting the roll-up process and effect of the relative strengths of the vorticity in the outer and inner flow regions of the wall jet in determining whether a dipole or mono-pole forms. They also noted that at low Reynolds numbers viscous diffusion acts quickly enough to prevent dipole formation.

The experiments of Tabaczynski *et al* (1970) document the transition of the piston vortex from laminar to turbulent and as mentioned earlier no transition mechanism was suggested. Experiments of Allen & Auvity (2002), investigating the effect of the piston vortex on the primary vortex generated at a tube exit, identified an instability on the piston vortex with a well defined wavelength. The instability appears to forming on the outer turn of the piston vortex. It was postulated that this instability was centrifugal in

nature and satisfied the criteria for instability of a wall jet on a concave surface, as described in Floryan (1986).
A similar instability phenomenon occurs in cavity flows. Cavity flows of sufficiently high Reynolds number display an instability that has been labeled Taylor-Gortler like (TGL) vortices by a number of workers , Koseff & Street (1984b), Kim & Moin (1985) and Aidun *et al* (1991). The mechanism for the formation of these instabilities has been attributed to the region of high shear that exists between the primary vortex and the viscous eddy, coupled with the curvature of the shear flow in this region. Linearised instability calculations of Ramanan & Homsy (1994) for a steady cavity flow indicate the that the region of high shear, between the primary inviscid eddy and the corner viscous eddies is responsible for the production of the Taylor-Gortler like cells observed in experiments. They computed that the separated region between the downstream eddy and the primary structure is where the first, long wavelength, instability mode appears. At a slightly higher Reynolds number, the separated region between the upstream secondary eddy and the primary structure is where a shorter wavelength centrifugal instability appears. Ramanan & Homsy (1994) note that as the Reynolds number increases the relationship between the amplification rate and corresponding wavelength becomes flatter, indicating the tendency for several modes to become unstable at once.
Koseff & Street (1984a) identified an instability forming on the growing corner structure, during start-up, that they classified as Taylor cells. They suggested that this instability was similar to that which forms on the surface of an impulsively started rotating cylinder, see Kirchner & Chen (1970). Koseff & Street (1984a) noted that the wavelength of this "start-up" instability was smaller that the TGL instability forming at the downstream secondary eddy and doubt exists as to the relationship between these two instabilities.

The current study will examine the formation of this transient structure in an experimental configuration where geometric length scales are absent to test for self-similar behavior. As previous experimental results have suggested a possible transition mechanism in terms of a centrifugal instability a detailed examination of this instability and its role in the transition to turbulence is a second focus of this study.

2. Experimental apparatus.

The experimental apparatus consisted of a 30cm wide, 150cm long moving belt. The belt was set in motion with a predetermined velocity characteristic using a programmable stepper motor. The belt was fully immersed in a water tank. The stationary plate consisted of an acrylic sheet, with an edge angle machined to 15 degrees. Attached to the edge was a 0.015 cm thick, 2.5 *cm* wide strip of thick brass shim stock. During experiments the shim stock was in contact with the moving belt and formed a junction with minimal step. It was important for the shim to be in contact with the moving belt, otherwise the presence of a small lip had the effect of promoting instabilities on the separated structure. A schematic of the apparatus is shown in figure 2. The dimensions of the apparatus ensured that the length scales of the vortical structure, 0.5-5*cm*, were almost an order of magnitude smaller than the width and depth of the facility. The moving belt was started impulsively and experiments were conducted in both water and air to achieve a large Reynolds number range. A Reynolds number based on the depth of the water

surface to the moving wall, Re_U, was 12 to 2570. This Reynolds number represents a way to differentiate wall speeds as it is expected that the length scale used does not play a role in determining the early characteristics of the vortex structure. The range of developing Reynolds number achievable with this apparatus was from Re_Γ=500 to 500,000. This large range of Reynolds number allows the observation of the transition of the structure from laminar to turbulent behavior.

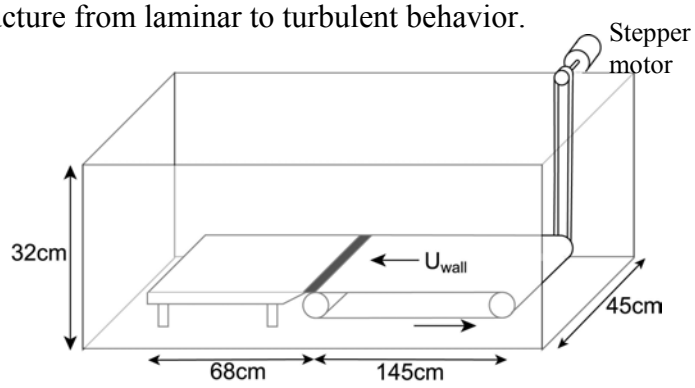

Figure 2 Experimental apparatus

For the experiments in water the fluid temperature was maintained at $22^o \pm 0.5^oC$ (laboratory temperature). Extreme care was required to have as small as possible temperature differential between the tank and surroundings as the vortex trajectory was found to be very sensitive to the presence of temperature induced convective motions. The experimental techniques involved generating a laser sheet in a plane perpendicular and parallel to the moving belt. Fluorescent dye and smoke were used to visualize the motion and size of the vortex core and Particle Image Velocimetry (PIV) data was collected to provide information about the unsteady streamline field and the strength of the vortex.

3. Results

3.1 Self-similarity of the junction vortex

An example of a laser cross section of the vortical structure using fluorescent dye is shown in figure 3, along with the core location, labeled as (X_Γ, Y_Γ). The origin of coordinate system is set at the junction of the moving wall with the stationary one, as shown in figure 3.

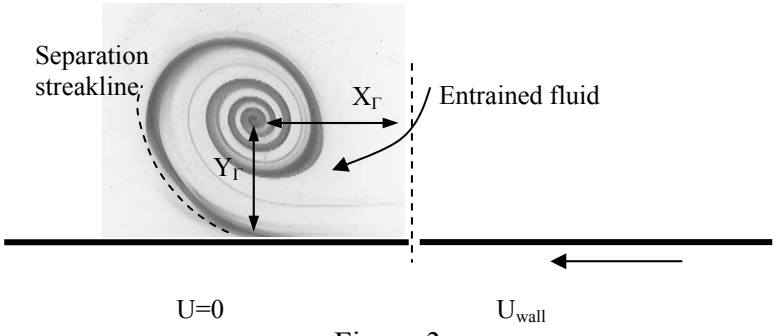

Figure 3

If the size of the vortex structure that forms close to the junction is an order of magnitude less than the external/apparatus length scale then one may expect that the structure scales in a self-similar fashion. Dimensional analysis then suggests that (X_Γ, Y_Γ) are functions of U_{wall}, t and υ only. Hence one can form the following non-dimensional groups to describe the vortex behavior $X_\Gamma/(U_{wall}t) = f_1(\mathrm{Re}_\Gamma)$ and $Y_\Gamma/(\sqrt{\upsilon t}) = f_2(\mathrm{Re}_\Gamma)$, where $U_{wall}^2 t/\upsilon = \mathrm{Re}_\Gamma$. $U_{wall}t$ represents a convective length scale L, the distance the wall has moved from rest and $\sqrt{\upsilon t}$ represents a viscous length scale. Re_Γ can be thought of a ratio of convective to viscous scales. Alternatively, if one considers the flux of circulation into the corner region as being proportional to $0.5U_{Wall}^2 t$ then Re_Γ can be though of as giving an indication of the strength of the separated structure. X_Γ has been scaled with respect to the convective scale as it represents displacement in the direction of wall motion. Y_Γ has been scaled with respect to the viscous length as the displacement of the structure away form the wall is a function of the growing boundary layer thickness. Figure 4(a) shows X_Γ / L scaled with respect to Re_Γ and figure 4(b) shows $Y_\Gamma / \sqrt{\upsilon t}$ scaled with respect to Re_Γ. The data in the plots in figure 4 are from experiments in air and water. Data sets for both these experiments show good universal collapse. From experiments it appears that the growth of X_Γ was far more susceptible to residual temperature induced convective motions than the data for Y_Γ.

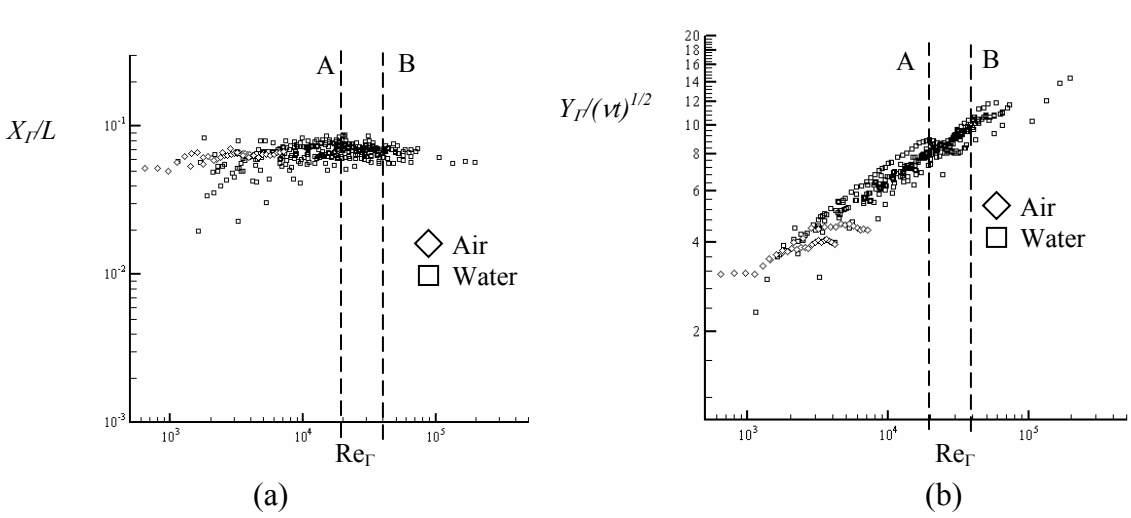

Figure 4

From figure 4 (a) it appears that the horizontal location of the vortex core, X_Γ, scales independently of Reynolds number, Re_Γ, allowing for experimental scatter. This means the structure scales in the horizontal direction as a function of wall speed only, a convective scale. A curve fit to the data gives $X_\Gamma / L \approx 0.07$, which implies $X_\Gamma \propto t$. The data for Y_Γ location of the vortex core, figure 4(b) also shows excellent universal collapse over a large range of Reynolds numbers. The data has a functional dependence on Re_Γ which appears to be of a power law form. Curve fits to the data give $Y_\Gamma / \sqrt{\upsilon t} = 0.4\,\mathrm{Re}_\Gamma^{0.3}$ and hence $Y_\Gamma \propto t^{0.8}$. This scaling rate is considerably faster than a

viscous scaling rate of $t^{1/2}$. The suggested reason for this is that inviscid entrainment is occurring into the vortex via the alleyway indicated in figure 3. The calculations of Conlon & Lichter (1995) suggested that if strength of the vorticity in the layer close to the wall is not of sufficient strength in relation to the outer layer of vorticity in the wall jet then a monopole structure forms. In time the monopole structure propagated toward the stationary wall rather than away. Conlon & Lichter (1995) suggested that the formation of a dipole structure was characterized by a roll-up of secondary vorticity and a divergence of the structure away from the surface. In the current experiments there is no indication of the roll-up of this secondary layer but there is a strong growth of the primary structure away from the wall, perhaps indicating the subtle effect of the time varying strength of vorticity that is being convected into the junction region from the Stokes layer. The data sets for the Y_Γ coordinate also show a trend to scale at a reduced rate toward the end of an experiment, especially for the lower unit Reynolds number cases. The suggested reason for this is that the size of the structure in the vertical direction is now of the order the depth of the facility and the presence of the boundary has had the effect of reducing the growth rate of the structure in the vertical direction. A similar phenomenon has been noted in the transient cavity study of Migeon *et al* (2000). Also shown in figure 4 is the point marked *A* where instability waves first begin to appear on the vortex structure and the point, *B*, where the vortex appears to be fully turbulent. Figure 5 shows the data for Y_Γ scaled with L versus Re_Γ. From figure 5 it is clearly evident that the Y_Γ coordinate does not scale with the convective length scale L. There also appears to be a significant divergence between the data sets for air and water. Again this would seem to confirm that the growth of the structure in the vertical direction is basically a viscous driven one.

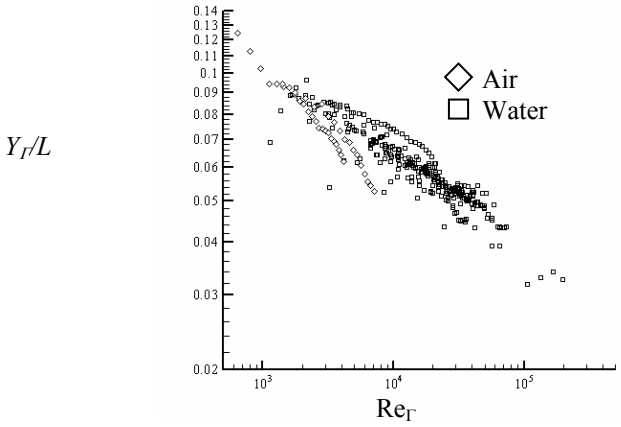

Figure 5

These results suggest that the structure scales in a self-similar fashion when Re_Γ is large but while the structure is still relatively small in relation to the apparatus length scale. Self-similarity scaling suggests that the shape of the structure is universal at identical developing Re_Γ for different Re_U. Figure 6 shows a selection of images of the developing structure for three different Re_U, at equivalent Re_Γ. The non-dimensional length scale shown in the images is $r^* = rU_{wall}/\upsilon$

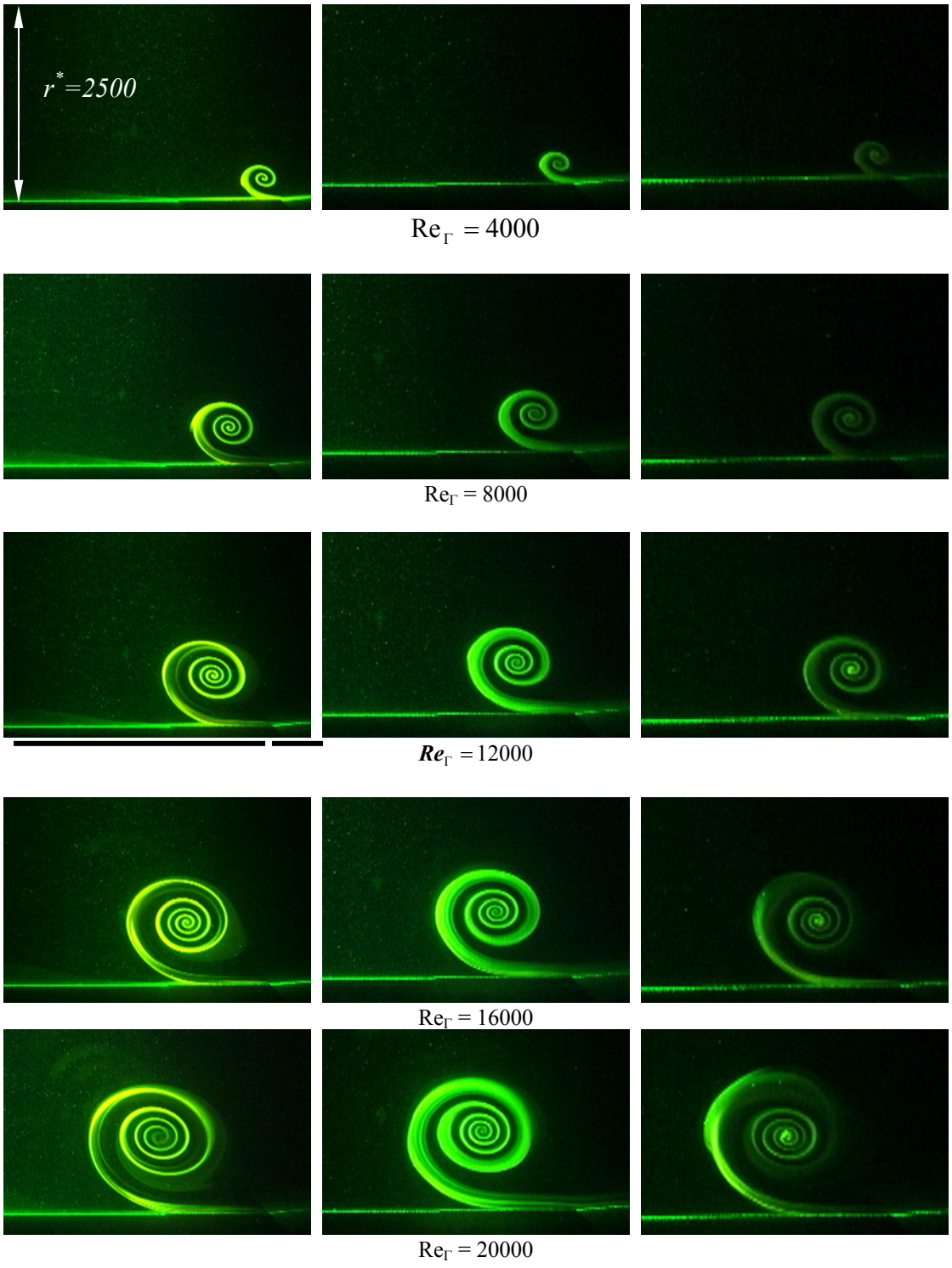

Figure 6. Development of the junction vortex for (a) Re_U =53,000, (b) Re_U =69,000 and (c) Re_U =103,000.

The images in figure 6 where obtained using fluorescent dye in water. An obvious indictor of the quality of the self-similarity is the shape and turns on the spirals for equivalent Re_Γ, while having very different physical scale differences. The structures shown for $\mathrm{Re}_\Gamma = 20{,}000$ are starting to show signs of instability on the outer turn of the streakline that demarcates the region of high shear between the rapidly rotating fluid whose origin is from the Stokes layer forming over the moving wall and the fluid originally located over the stationary wall that is being displaced slowly to the left. This is a sign of the development of a centrifugal instability that will be discussed in section 3.5 and is marked by the location of the vertical line *A* in figure 4(a) and (b). The "separation" point on the stationary plate appears to be moving along the plate and located directly below the primary vortex core. It would be expected that this point represents the region of maximum adverse pressure gradient on the plate. Unsteady separation is characterized by the Moore-Rott-Sears condition that there is a point, not necessarily on the no-slip boundary for which $\partial u / \partial y = 0, u = 0$. During the execution of these experiments it was noted that if the junction between the plate and belt was poor, i.e. a gap existed or the thickness of the lip on the stationary plate was of order the boundary layer thickenss, a Kelvin-Helmholtz like instability would appear on the outer turn of the vortex. By making the lip from thin shim stock and having it in continual contact with the moving plate this instability was suppressed. .

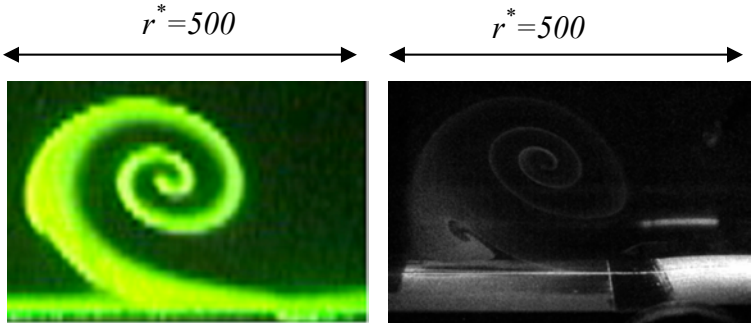

(a) (b)

Figure 7 Experiments in (a) water, $\mathrm{Re}_U = 530$ and (b) air $\mathrm{Re}_U = 69$ for $\mathrm{Re}_\Gamma = 4000$

Figure 7 shows a comparison between a fluorescent flow visualization in water and a smoke visualization in air. The purpose of these images is to show the similarity in structure for the vortical structure using fluids of two differing viscosities, at relatively high Re_Γ and a large difference in physical scales, ~8x. In figure 7(b) a region of fluid with opposite signed rotation to the primary structure can be seen. This rotation represents the secondary vorticity that is formed on the stationary wall in response the convection of primary vorticity from the moving wall. It does not appear that there is any region of "reversed" flow over the stationary wall. This is confirmed with PIV data presented in section 3.2 and similar behavior was noted in the experimental study of Lichter et al. (1992).

3.2 Development of the junction vortex topology

PIV experiments were performed to generate quantitative velocity and vorticity information during the development phase. The data acquisition system consisted of an argon ion laser, an externally triggered Cohu 6600-3000 series full frame transfer video camera, 659 x 496 pixels, with 10 bit resolution, a General Scanning 6120DT series oscillating mirror and an Epix frame grabber. Details of the PIV system hardware and software, capable of producing at time difference between images of the order 0.5 *ms,* are contained in Allen & Smits (2001) Figure 8 shows a sequence velocity fields for Re_U = 520. The defining feature of these patterns is the developing rotational core as the boundary layer from the moving wall separates and penetrates into the quiescent fluid. The region of high shear between the separating wall jet and the stationary wall is evident from the velocity field and is highlighted in figure 8(e). It also can be seen that there is no region of reversed flow over the stationary plate. As is the case with the dye spirals, the quantitative features of the streamline patters appear to be self-similar. Lichter et al (1992) also produced a similar velocity field while they were injecting a jet of fluid into a tank to model a separating coastal current and noted the lack of reversed flow over the stationary wall despite the presence of strong secondary vorticity.

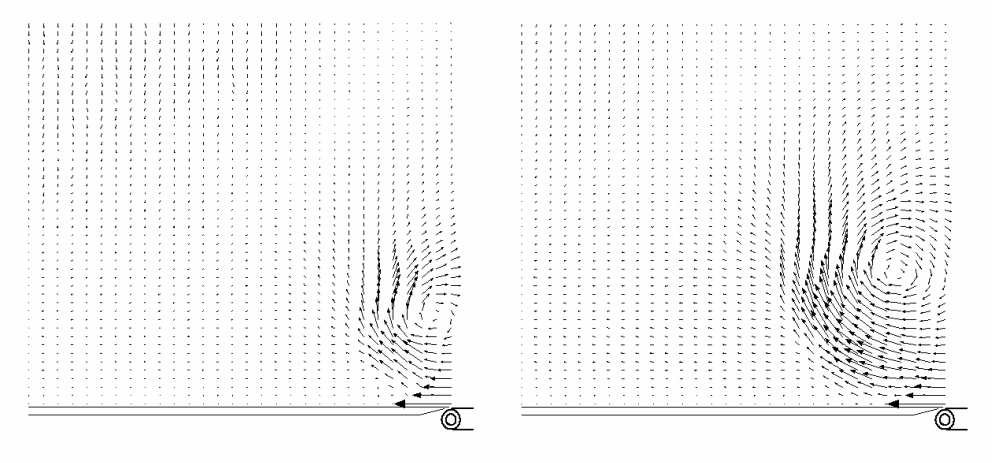

(a) $\boldsymbol{Re}_\Gamma = 2000$ (b) $\boldsymbol{Re}_\Gamma = 4000$

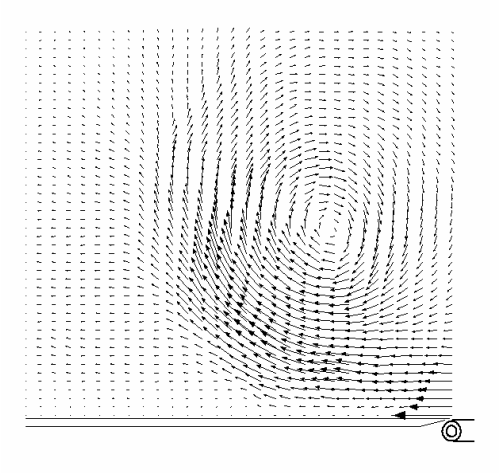

(c) $\mathrm{Re}_\Gamma = 8000$

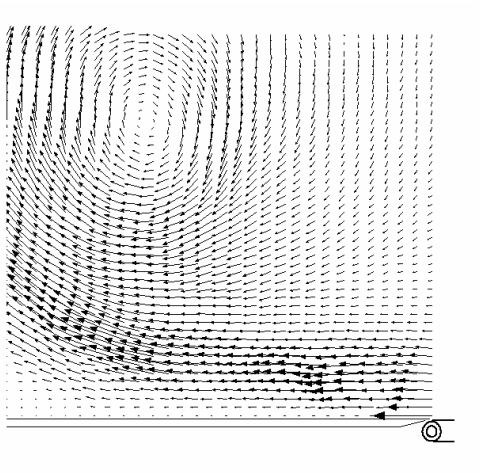

(d) $\mathrm{Re}_\Gamma = 12000$

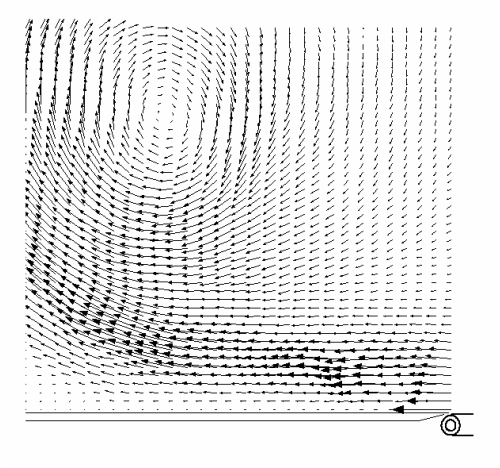

(e) $\mathrm{Re}_\Gamma = 16000$

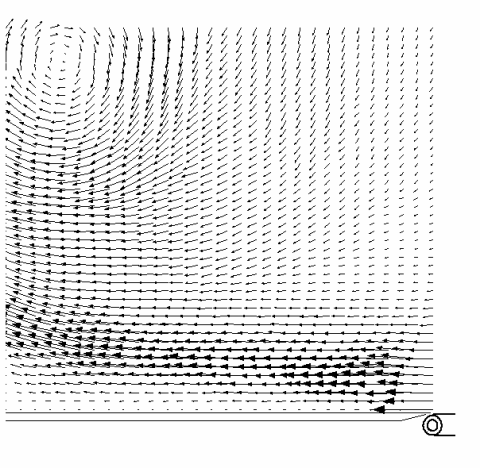

(f) $\mathrm{Re}_\Gamma = 20000$

Figure 8 Velocity field development for $\mathrm{Re}_U = 520$

Figure 9 shows the development of the vorticity field for the same sequence of velocity fields in figure 8. The plots show non-dimensional vorticity, $\omega = \Omega\upsilon / U_{wall}$.

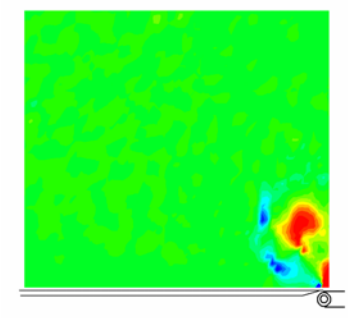

(a) $\mathrm{Re}_\Gamma = 2000$

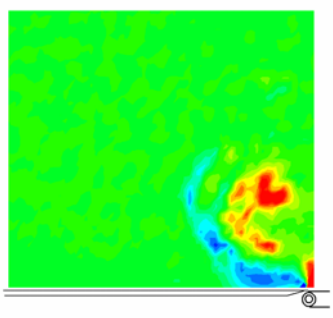

(b) $\mathrm{Re}_\Gamma = 4000$

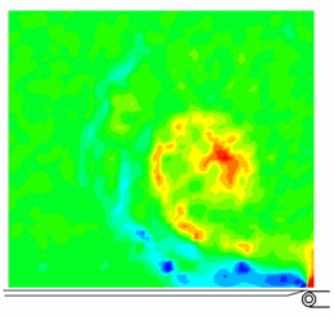

(c) $\mathrm{Re}_\Gamma = 8000$

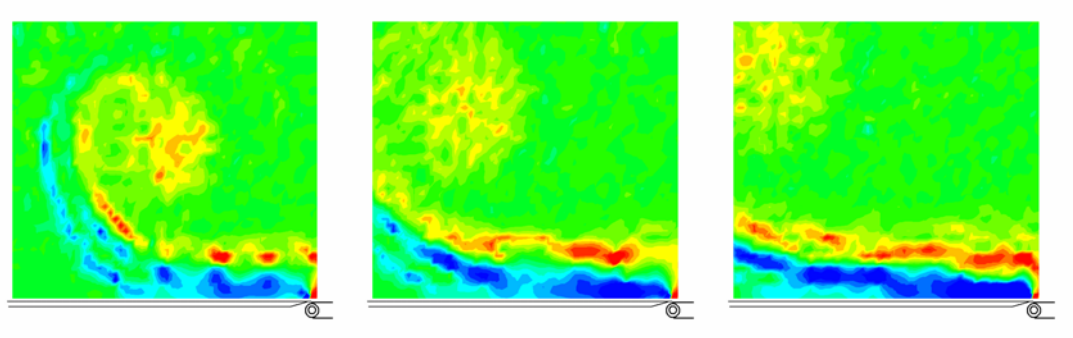

(d) $\mathrm{Re}_\Gamma = 12000$ (e) $\mathrm{Re}_\Gamma = 16000$ (f) $\mathrm{Re}_\Gamma = 20000$

Figure 9 Vorticity field development for $\mathrm{Re}_U = 520$

The vorticity profiles show two important features. The rolling-up of the boundary layer material from the moving wall into a coherent spiral of vorticity, similar in form to that measured by Allen & Chong (2000) and the production of strong secondary vorticity on the stationary plate. As mentioned earlier the secondary vorticity is generated in order to preserve the no-slip condition over the stationary plate and indicates the presence of a strong adverse pressure gradient along the stationary plate. The secondary vorticity appears to be wrapping around the periphery of the main primary structure as the structure moves along the stationary wall. The experiments of Lichter *et al* (1992), using particle tracking to study the formation of large separated coastal eddies, measured a concentrated region of primary vorticity, with a secondary vorticity plume, generated at the stationary surface, being wrapped around the primary core. The computations of Conlon & Lichter (1995) also show a similar effect, namely *"a region of highly stretched negative vorticity wrapping around the dominant eddy"* when their vorticity ratio was less than 0.5. The vorticity ratio is defined as the ratio of the maximum negative to positive vorticity at the wall jet inlet. The vorticity distributions do no show any evidence of dipole formation which occurs when the secondary vorticity rolls into a coherent structure, similar in form to that seen in vortex rebound experiments of Walker *et al.* (1987) and the computations of Orlandi & Verzicco (1993)

3.3 Formation Mechanism

An obvious question that arises from this study is "what is the formation criteria for the vortical structure?". From experiments in water it appeared that formation, based on observation of the streak line rotating at $\mathrm{Re}_U \approx 100$ in water and $\mathrm{Re}_U \approx 60$ in air. A particular "time" at which the structure first appears was not apparent. Perhaps the simplest description as to why vortex roll-up occurs comes from consideration of the Stokes layer as a front of vorticity entering a quiescent fluid. Stern & Pratt(1985), using an inviscid analysis, calculated that the leading edge of the structure, the nose, is robust however behind the leading edge the possibility exists for folding of the front due to an inflectional instability that results in a structure that appears similar in form to a starting vortex, as shown in figure 10.

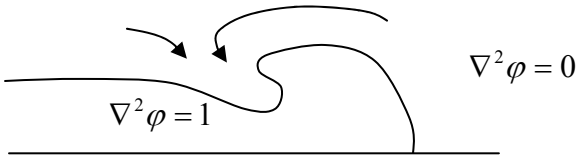

Figure 10 distortion of a vorticity front from Stern & Pratt(1985).

At very early time one would imagine the problem is viscous dominated and the flow topology should be implied from an unsteady Stokes solution before transitioning to a high Reynolds number solution. Cantwell (1986) considered the transient motion of a viscous fluid forced from an initial state of rest in an effort to clarify the events leading to the creation of a starting vortex at the head of a jet. By describing the motion in terms of viscous similarity variables he was able to deduce critical Reynolds numbers for bifurcations in a planar jet structure where the evolving jet front begins to display a lead vortex structure. This represents the time at which the critical points in the entrainment diagram change form being a off-axis stable nodes to stable foci. The parameter describing the bifurcation is a Reynolds number based on the time varying impulse that is being applied to the initially quiescent fluid, defined as $\mathrm{Re}_I = [I(t)t]^{2/3}/(4\upsilon t)$. The momentum source for the jet in this study was a point source. The critical Reynolds number for a constant rate of momentum, plane jet was $\mathrm{Re}_I = 2.2$ and for a plane jet with a constantly increasing rate of momentum injection $\mathrm{Re}_I = 1.2$

The point source on momentum injection and lack of fixed wall are of course different boundary conditions than in the current experiment, however many of the features of the current study display starting jet characteristics. A crude approximation for the momentum of the fluid being ejected from the moving wall can be made using Stokes description for the velocity of fluid developing over a wall started from rest as $I(t) \approx t^{3/2}$. Indicating the impulsively started belt, in the far field, appears to have characteristics lying between a plane jet and ramped jet. Hence based on the critical Reynolds numbers of Cantwell (1986) we have a combination of wall speed and viscosity for the appearance of a jet like structure of $0.4U_w^{4/3}t^{2/3}/\upsilon^{2/3} \approx 2$. This relationship would suggest the formation of the monopole structure is dependent on wall speed, viscosity and time. Typical formation times, based on current experimental configurations would be of the order 0.01sec for a wall speed of 30mm/sec in water and 0.05sec for the experiments in air with a wall speed of 60mm/sec. This physical time scale is very brief and hence the apparent reason why the vortex appears to be present as soon as the belt is set in motion. The effect of the stationary wall will be to effectively reduce the overall impulse applied by the moving belt to the flow field and hence the stated times are likely to be an underestimate for the critical formation time. Cantwell (1986) notes that in the case of the viscous vortex ring, the time evolving Reynolds number decreases with time, after the initial impulse is applied to the fluid. This means that if a time line interacts with the vortex after the Reynolds number has dropped below the critical Reynolds number for the presence of a stable focus in the entrainment diagram, no roll-up of the line will occur. It does appear from the current experiments that there is a wall speed, below which the dye

line does not roll back on itself, hence the jet front is not developing an inflexional instability. Conlon & Lichter (1995) also suggested a lower limit on Reynolds number for dipole formation of $\mathrm{Re} \approx 50$. The mechanism for suppression of diploe formation was stated as the action of viscosity. The Reynolds number in this case was based on the wall jet speed and the width of the jet. This Reynolds number represents the flux of the jet. Using a Stokes layer description for the incoming jet, results in an expression for the unsteady Reynolds number, below which a monopole will not form of $\mathrm{Re}_\Gamma < 1400$, which is close to what can be resolved experimentally, see figure 4. A consequence of Cantwells formulation is that a lead vortex will always form if the rate of momentum being injected into the flow is equal to or exceeds t^p where $p > -1/2$. For the Stokes layer we approximated $p = 1/2$. It may be possible to reconcile to model of Cantwell (1986), the computational results of Conlon & Lichter (1995) and the current experimental results by hypothesizing that the action of the secondary vorticity is to remove momentum form the flow at such a rate that prevents the critical Re_l from being reached.

Literature related to an analytical solution in the corner region is limited to steady flow analysis and as such does not provide any information on the unsteady separation mechanism. The nature of the steady flow solutions from Hancock et al (1982) and Taylor (1962) resemble in a qualitative sense the experimental results after the initial transient has formed and passed. As mentioned earlier, Taylor (1962) calculated a steady viscous solution and Hancock et al (1982) generated an inertial expansion. The solution of Hancock et al (1982) is interesting in that they reference the fact that the boundary layer over the stationary surface appears to be "wall jet" in nature. Examination of this analytical solution in the region $5 \approx r^*$, over the stationary wall, shows that the strength of the vorticity in the wall bounded section of the wall jet is in fact stronger in peak strength than the outer layer. Based on the conditions suggested by Conlon & Lichter (1995) one would expect the formation of a dipole, or at lest the movement of the structure away from the stationary surface.

4 Instability development

4.1 Instability wavelength

At $\boldsymbol{Re}_\Gamma \approx 13{,}000$ waves begin to appear on the outer turn of the vortex structure, as illustrated in figure 11(a). The amplification of these waves leads to the eventual transition to a turbulent structure at $\boldsymbol{Re}_\Gamma \approx 40{,}000$. Figure 11(b) shows what appears to be a fully turbulent vortex at $\boldsymbol{Re}_\Gamma = 109{,}000$. Transition to turbulence of the vortex in front of a piston in a cylinder was remarked on by Tabaczynski et al (1970) but no detailed description of a transition mechanism was provided. Similar unstable waves have been observed by Allen & Auvity (2000) on the vortex forming in front of a moving piston. In the context of start up cavity flow experiments Kosseff & Street(1984a) noted that during the start-up or initial transient period that the junction vortex, described as a "cylinder of high vorticity fluid" became unstable, developing torroidal vortices on its periphery. The suggested mechanism for this was that of a Taylor instability. They noted that the wavelength of the instability decreased as the belt speed increased. A similar

phenomenon of wavelength reduction with belt speed has been observed in the current experiments.

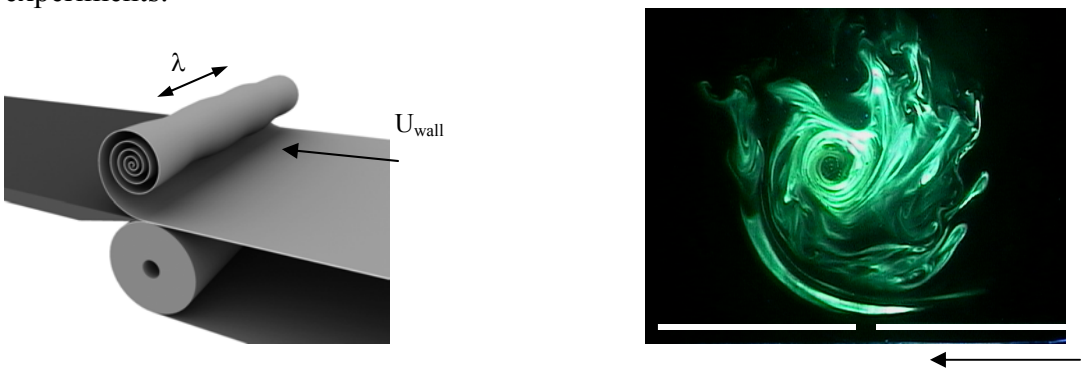

(a) (b)

Figure 11

In order to examine the detailed structure of the instability, a laser cross-section was taken in a plane inclined at 43° to the plate, as shown in figure 12(a). This was done in order to have the vortex core in the visualization plane for as long as possible. Fluorescent dye was placed along the edge of the stationary plate before the wall was set in motion. A typical image of a spanwise cross section through the vortex core is shown in figure 12 (b)

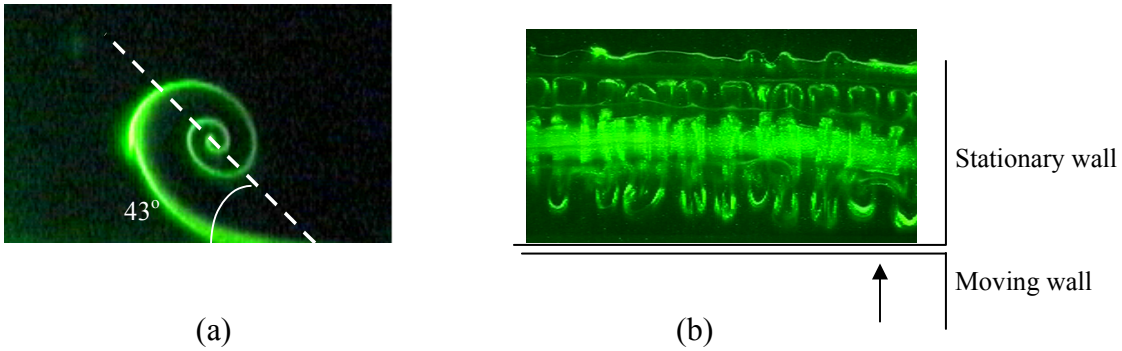

(a) (b)

Figure 12

The instability waves appear on the outer turn of vortex and are ingested into the vortex core. The presence of these mushroom structures would suggest a significant reorientation of the spanwise vorticity into streamwise filaments. As time increases the amplitude of waves increases. The non-linear growth of these waves eventually results in the breakdown of the primary core. Significant care had to be taken during execution of experiments as the instability growth rate and wavelength are sensitive to background disturbances. Once the structures have formed, the wavelength does not vary as time increases. This observation implies that a range wavelengths can be excited with a small variation in experimental conditions. Once a wavelength has been established it dominates the flow. It does appear that there is a finite bandwidth for the disturbances.
As the Re_U increases, the wavelength of instability becomes shorter.

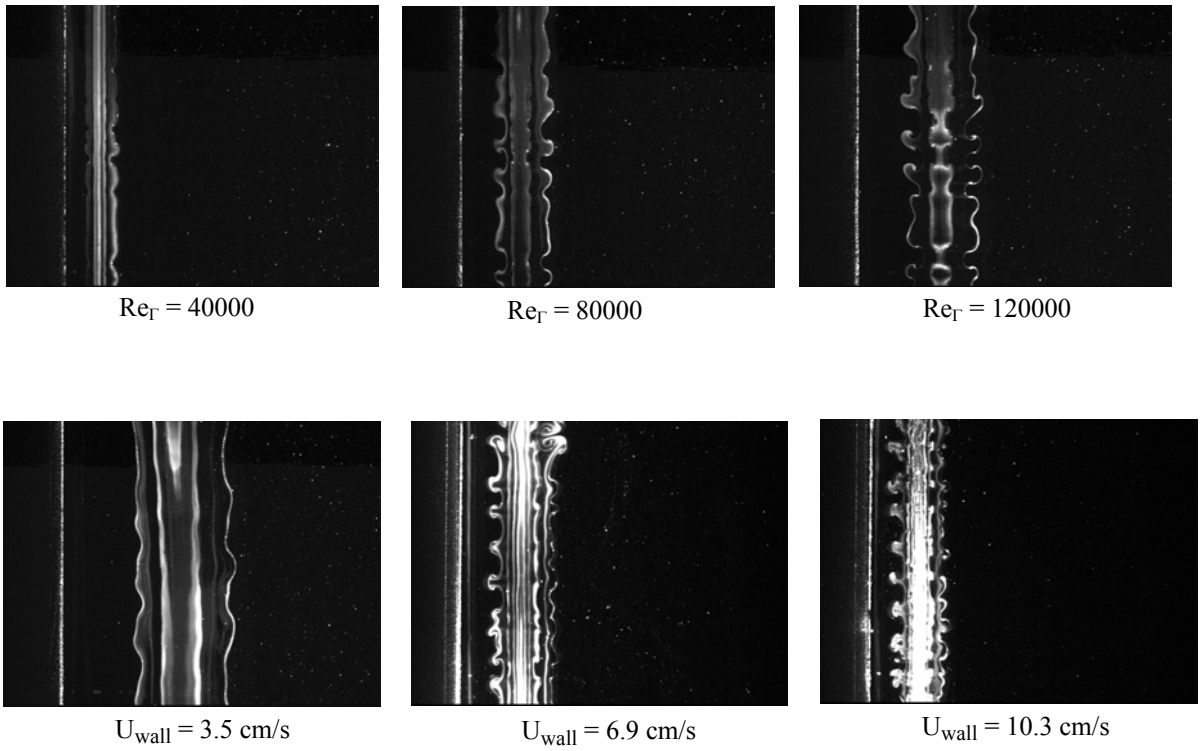

Figure 13

Figure 13 shows instability waves at Re_Γ = 12000 for three different Re_U. The minimal unit Reynolds number where a junction vortex is formed is approximately 40. In the range of Re_U from 40 to 300 the instability wave is hard to detect as the structure extremely sensitive to background disturbances. In the range of Re_U from 300 to 1030, the development process is relatively easy to measure.

In order to measure the spatial scale of these instability waves, the location of the wavy streak line profile, on the outer turn of the vortex, was obtained from images such as figure 13. This data was processed with a discrete Fourier transformation to extract wavelength information. The range of wavenumber is somewhat scattered due to the irregularity of the streakline profile, though wavenumber data does not change as Re_Γ increases for a given experiment. Figure 14 shows data for the amplified wavelength, normalized with respect to U_{wall} and υ, plotted with respect to Re_U. The data shows a relative insensitivity to Re_U. The error bars indicate the scatter in range of wavelengths. It can be seen that the trend is for wavelength to decrease as the wall speed increases.

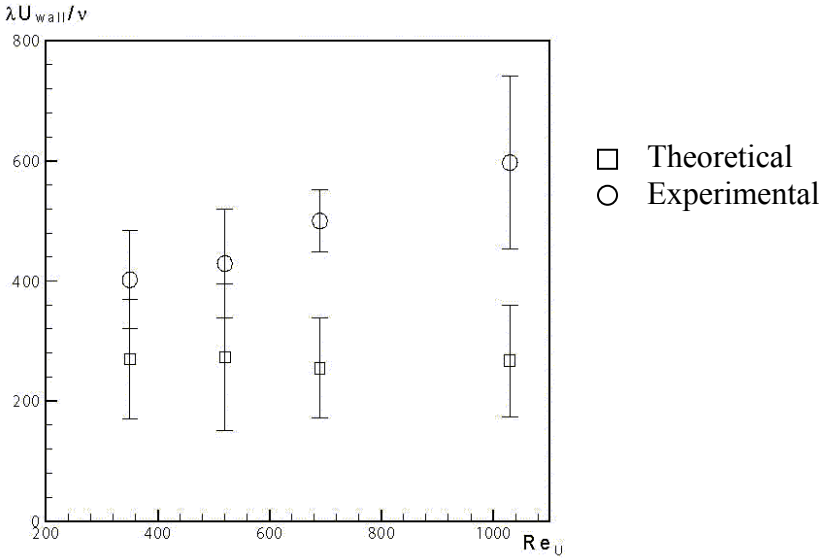

Figure 14

4.2 Instability strength

PIV measurements were performed in a plane parallel with the axis of the primary core, indicated by the slice shown in figure 12, to determine the strength of these instability structures. In this experiment the location of the vortical structures was "locked" spatially by a series of small 0.2mm high bumps on the blade edge. As the wavelength of the structures is sensitive to background disturbances they are lock well to a known spatial disturbance.

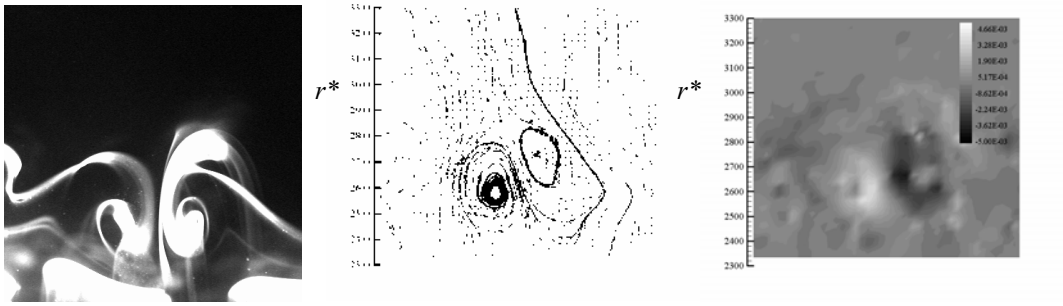

(a) (b) (c)

Figure 15

Figure 15(a) shows a flow visualization image of the vortical structure on the outer turn of the primary vortex. Figure 15(b) and (c) show the corresponding streamline pattern and vorticity field. The vorticity Ω has been normalized with respect to U_{wall} and υ. The peak strength of the instability is of the same order as the peak vorticity measurements in figure 9. This would indicate a significant re-orientation and stretching of the vorticity has occurred on the separating vortex sheet.

4.3 Instability mechanism

As mentioned in the introduction this type of flow has topology and boundary condition similarities with cavity flows, hence it would seem logical to look to the stability of cavity flows for elucidation of the mechanism of the instability observed in the current experiments. Instability discussion in relation to cavity flows has typically revolved around the role of the downstream secondary eddy rather than the effect of the corner singularity. Koseff & Street (1984a) drew a clear distinction between the downstream Tayler-Görtler-Like (TGL) instability in a cavity and the transient instability forming on the primary vortex. This provoked considerable interest from one reviewer who commented that the instabilities may be the same, a manifestation of a centrifugal instability (J.A.C. Humphrey). A second reviewer (A.Pollard) questioned the source of the instability and suggested that its origin may be from the corner singularity, rather than the separating shear layer. Koseff & Street (1984a) responded that the Taylor cells may be important in establishing the TGL but not responsible for their continued presence as there was no evidence of an instability close to the corner junction in the steady state and that the wavelength of the TGL instability was in general longer, compared to the start-up instability, for a given Reynolds number. As mentioned, the mechanism for the generation of TGL vortices near the downstream secondary eddy in cavity flows appears to be fairly well understood. Ramanan & Homsy (1994), using a linerarized instability calculation stated that "*the dividing streamline between the primary vortex core and the downstream secondary eddy is the source of disturbance energy. There is an unstable stratification of centrifugal force associated with the free shear layer near the dividing streamline which approximates the flow on a concave wall*". The sensitivity of wavelength selection mentioned by Ramanan & Homsy (1994) would seem to have been confirmed by the experiments of Guermond *et al* (2002) who were able to vary the wavelength of the TGL cells by as much as 100% via the introduction of small disturbances near the junction between the moving plate and stationary surface. This would seem to discount the conjection of Koseff & Street (1984a) that the transient instability is not important in terms of wavelength selection and imply that the source of the instability wavelength is near the junction singularity. A further point from the study of of Guermond *et al* (2002) was that for an Re=1000, they noted the beginnings of the formation of rotational cells on the downstream wall, in a region where separation had not occurred and concluded that the instability is not induced by separation, but it is rather a Taylor-Couette-type instability. This is somewhat in agreement with the conjecture of A.Pollard, a reviewer of Koseff & Street(1984a)

From flow visualization experiments it appears that the instability has its source on the outer turn of the primary vortex. In order to construct a physical mechanism for the generation of these structures one must consider how the corner vortex is being generated. Figure 16 shows a velocity field in the corner region and overlaid on this plot is an individual velocity profile in the separated region.

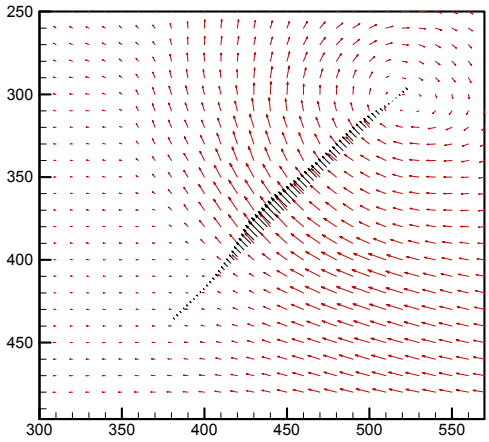

Figure 16

As mentioned previously, the process of formation of this structure is that when the belt is set in motion, a Stokes like boundary layer forms on the moving belt. The boundary layer is then convected over the stationary plate, resulting in the production of significant secondary vorticity on the stationary plate. This structure then separates, resulting in a velocity profile that resembles "wall jet" subject to concave curvature. A wall jet subject to concave curvature is unstable due to the presence of centrifugal forces, see Floryan & Saric (1984). It is in the inner flow, the section of the flow between the wall and the point of maximum velocity, that the instability will first develop in a wall jet subject to concave curvature. The control parameter for this type of flow is the Görtler number, $Go = U_\infty \delta / \upsilon \times \sqrt{\delta / R}$, where U_∞ is the maximum velocity of the wall jet, R is the radius of curvature and δ is the wall jet thickness. A criterion for the development of Görtler vortices in the wall jet with concave curvature is $Go > 1.0$. There is no critical wavenumber and the characteristics of the vortices are determined by the disturbance growth process. Experiments to determine the natural wavelength of Görtler vortices have been found to be extremely sensitive to the properties of the apparatus and its flowfield, see Tani & Sakagami (1964). Bippes(1978) recorded the wavelength of the Görtler as being that of the highest amplification rate from linear theory and once the wavelength is established it is preserved during downstream development of the cells.
To support the argument that the instability is Taylor-Görtler in form an attempt has been made to compare the wavelength of a junction vortex with that of theoretical prediction on the Görtler instability. Floryan(1986) argues that the most amplified wavelength changes with Görtler number by means of a dimensionless wavelength parameter Λexpressed as follows, $\Lambda = F^{1/3} \lambda^{1/3} \nu^{-1} \left(\lambda / R\right)^{1/2}$. Here F is the dimensional "flux of external momentum flux", see Glauert (1956), λ is the dimensional wavelength, ν the kinematic viscosity, R the radius of a wall curvature. Floryan (1986) showed that the values of Λ for the maximum amplification rate are in the range of 48 to 85, when Görtler numbers vary from 5 to 20 respectively. F can be calculated from the velocity profile obtained by means of the PIV results with $F = \int_0^\infty u \left(\int_y^\infty u^2 dy \right) dy$. Substituting

experimental data for the velocity profile to this equation λ can be estimated and is plotted in figure 14. Although there is an element of error in selection of the velocity profile to use, the wavelength from experiments and the theoretical predictions of Floryan (1986) are the same order and show similar trend, hence it is reasonable to conclude that the mechanism of the instability of the junction vortex is Görtler in nature due to the presence of centrifugal forces. Floryan(1989) also provides information on the spatial growth of the Görtler structures, however correlation with experimental data is hard due to experimental error in estimation of Go and the size of the disturbance. The non-linear growth of the instability follows a similar non-linear growth mechanism outlined by Lasheras *et al.* (1986). They presented a physical model for the generation of the streamwise structures via non-linear vortex stretching and tilting in the highly strained braid region of a shear layer.

5. Conclusions

Detailed experiments have revealed the self-similar nature of the vortical structure that is formed in the region where a moving wall slides past a stationary one. This results in an unsteady front of vorticity, which is generated over the moving wall, being convected over the stationary one. The suggested mechanism for roll-up is that this vorticity sheet develops an inflectional instability, with the corner only being important in terms of setting up the conditions on the stationary plate for the formation of a wall jet. The reasons for the movement of the structure away form the surface is related to the presence of strong secondary vorticity on the stationary plate, formed in the near wall region of the wall jet. It has been suggested that the question as to whether a dipole structure forms or not is dependant on the rate of loss of momentum via the action of the stationary wall.

The instability that forms on the outer turn of this structure has been quantified with flow visualization and PIV. The instability was found to be extremely sensitive to disturbances and scales with velocity. The instability appears to be Görtler in nature. Using experimental data fields to make an estimate of the most unstable modes based on linear stability results gives reasonable correlation with experimental results for the observed wavelengths. The eventual non-linear growth of these structures results in the eventual turbulent breakdown of the structure.

6 References

Ahlnas, K. , Roger, T.C. and George, T.H. 1987 Multiple dipole formation in the Alaska Coastal Current detected with Landsat. *J. Geophys Res*. **92**, 13041-13047

Aidun, C.K. , Triantafillopoulos, N.G. and Benson, J.D. 1991 Global stability of a lid driven cavity with throughflow:Flow visualization studies. *Phys. of Fluids* **3** (9) 2018

Allen, J.J. & Chong, M.S. 2000 Vortex formation in front of a piston moving through a cylinder, *J.Fluid Mech,* **416,** 1-28.

Allen,J.J. and Auvity, B. 2002 Interaction of a vortex ring with a piston vortex, *J.Fluid Mech.* 2002, **465**, 453-378

Allen, J.J. & Smits, A.J. 2001 Energy Harvesting Eel. *J. Fluids and Structures* **15**, 629-640

Batchelor, G.K. 1967 *An Introduction to Fluid Dynamics*. Cambridge University Press.

Bajura, R.A. and Catalano, M.R. 1975 Transition in a two-dimensional plane wall jet *J. Fluid Mech*. **70**, 773-799

Burggraf,O. 1966 The structure of steady separated flows. *J.Fluid Mech.* **24**,113-151

Cantwell, B.J. 1986 Viscous starting jets. *J. Fluid Mech.,* **173,** 159-189

Chun, D.H. and Schwarz, W.H. , 1967 Stability of plane incompressible viscous wall jet subjected to small disturbances *Phys. Fluids* **10**, 911

Daneshyar, H., Fuler, D.E. and Deckker, B.E.L. 1973 Vortex motion induced by the motion of an internal combustion engine. *Intl. J. Mech. Sci.* **15**, 381-390

Floryan, J.M 1986 . Gortler Instability of boundary layers over concave and convex walls. *Phys. of Fluids* **29**(8) , 2380

Guermond, J.-L., Migeon,C. Pineau,G. and Quartapelle, L. 2002 Start up flows in three dimensional rectangular of aspect ratio 1:1:2 at Re=1000. *J.Fluid Mech.*, **450**, 169-199

Hancock, C. , Lewis, E. and Moffatt,H.K. Efects of inertia in forved corner flows 1981 *J.Fluid Mech.,* **112,** 315-327.

Kim,J. and Moin, P. 1985 Application of a fractional -step method to incompressible Navier -Stokes Equations. *Journal of Computational physics*, **59,** 308-323.

Pan, F and Acrivos, A. 1967 Steady flow in rectangular cavities. *J.Fluid Mech*, **28**, 643-655.

Kirchner, R.P and Chen, C.F. 1970 Stability of time-dependent rotational Couette flow. Part 1. Experimental investigation. *J.Fluid Mech.*, **40**, 39-47

Klein, R. Botta, N , Schneider, T, Munz,C.D. Roller,S. Meister,A , Hoffmann, L. Sonar,T. 2001 Asymptotic adaptive methods for multi-scale problems in fluid mechanics. *J. Eng. Math.* **39**, 261-343

Koseff, J.R. and Street, R.L. 1984 Visualization studies of a shear driven three-dimensional recirculating flow. *J Fluid Eng*, **106**, 21

Koseff, J.R. and Street, R.L. 1984 The Lid-driven cavity flow: A synthesis of qualitative and quantitative observations. *J. Fluids Eng,* **106**, 391

Koseff, J.and Street, R.L. the lid -driven cavity flow:A synthesis of qualitative and quantitative observations. 1984 J. Fluids Eng., **106**, 390-398

Lichter, S. , Flor J-B, and van Heijst G.-J. F. 1992 Modelling the separation and eddy formation of coastal currents in a stratified tank. *Exps. In Fluids*. **13**, 11-16

Migeon, C. Texier, A. and Pineau, G. , 2000 Effects of lid-driven cavity shape on the flow establishment phase. *J. Fluids and Structures* **14**, 469-488

Moffatt, H.K. Viscous and resistive eddies near a sharp corner,1964 *J.Fluid Mech*. **18** 1-18.
Obokata,T. and Okajima, A. 1992 Roll-up vortex on the reciprocating piston in a cylinder. *Sixth Intl. Symp.* On flow Visualization. (ed. Y. Tanida & H.Miyashiro), 594-598 Springer
Orlandi, P. and Verzicco, R., 1993, Vortex rings impinging on walls. *J.Fluid Mech* **256***,* 615-646
Tabaczynski, R.J., Hoult, D.P. and Keck, J.C. 1970 High Reynolds number flow in a moving corner, *J. Fluid Mech.* **42**, 249-255.
Taylor, G.I. 1960 *Aeronautics and Aeromechanics*. Pergamon Press
Ramanan, N. and Homsy, G.M. 1994 Linear Stability of lid-driven cavity flow. *Phys. of Fluids* **6** (8), 2690
Stern, M. E and Pratt, L.J., 1985, Dynamics of vorticity fronts. *J. Fluid Mech*, **161**, 513-532.
Walker, J.D.A., Smith, C.R., Cerra,A.W. and Doligaski, T.L., 1987, The impact of a vortex ring on a wall. *J. Fluid Mech.* **181**, 99-140